2025年臺灣國際科學展覽會
優勝作品專輯

作品編號　100045

參展科別　工程學

作品名稱　The Future of Carbon Capture Technology: A Novel Moisture Powered Thin-Film Supercapacitor that Adsorbs Carbon Dioxide

得獎獎項　一等獎

就讀學校　Daegu International School
指導教師　JAEHEE JANG
作者姓名　HANSEO KIM

關鍵詞　Carbon Capture, Moisture-Electricity Generation, Supercapacitive Swing Adsorption

作者照片

The Future of Carbon Capture Technology: A Novel Moisture Powered Thin-Film Supercapacitor that Adsorbs Carbon Dioxide

Hanseo Kim[1]

[1]**Daegu International School, Daegu, Republic of Korea**

Abstract - Carbon capture and storage technology (CCS) has tremendous potential to enable the use of fossil fuels while reducing the emissions of CO_2 into the atmosphere, and consequently combating climate change. CCS faces several challenges such as energy consumption, cost, low practical applications and environmentally friendliness. This research presents the first carbon capture device capable of capturing CO_2 while generating green energy. By integrating advanced materials science with sustainable energy principles, the device addresses the dual challenges of CO_2 mitigation and renewable energy production in a single, cost-effective platform. Beyond its technical innovations, this research highlights the device's scalability and potential to revolutionize carbon capture deployment. The device can be integrated into industrial emissions systems, transportation systems, urban infrastructure, or even wearable technologies, providing versatile applications across different sectors. Furthermore, the device's lightweight and flexible form factor ensures accessibility as it improves the applicability of CCS technology in remote or developing regions. This study demonstrated a novel approach to carbon capture by implementing carbon capture into a thin-film moisture electricity generator. The developed thin-film supercapacitor successfully demonstrated the capacity for supercapacitive swing adsorption of CO_2, which is a relatively novel approach to CCS that is cheap, environmentally friendly, and efficient while generating green energy from ambient humidity.

Key Words : Carbon Capture, Moisture-Electricity Generation, Supercapacitive Swing Adsorption

1. Introduction

Rising global temperatures and the pollution caused by fossil fuel has attracted global attention, and carbon dioxide (CO_2) produced from burning fossil fuels is one of the main causes of global warming [1-4]. Even with significant progress in renewable energy technologies, the usage of fossil fuels remains the dominant sources of the world energy production [5]. One promising technology to mitigate CO_2 emissions is carbon capture and storage (CCS). CCS technology reduces the atmospheric CO_2 levels by capturing, compressing and storing high concentrations of CO_2 [6]. Compared to other CO_2 mitigation technologies such as renewable energies, CCS is important as it serves as a strong short-term solution to the continued emission of greenhouse gases by decreasing CO_2 emissions until we can shift to a low carbon economy [7]. Today's industrially available CCS technology is solvent scrubbing, which utilizes amine solutions to selectively adsorb CO_2 [8]. This process, however, requires substantial energy as the solvent needs to be heated to release the adsorbed CO_2 to return to its original state. Other CCS technologies, such as solid adsorption has limitations in energy usages, membrane separation has limitations in service life and low selectivity, cryogenic separation has limitations in high operating costs, and the hydrate method has limitations in practical applications [9-12]. Therefore, electrochemical swing adsorption, a CCS technology that is driven by electrochemistry, is emerging as a cheap, environmentally friendly, and sustain-able alternative [13-15].

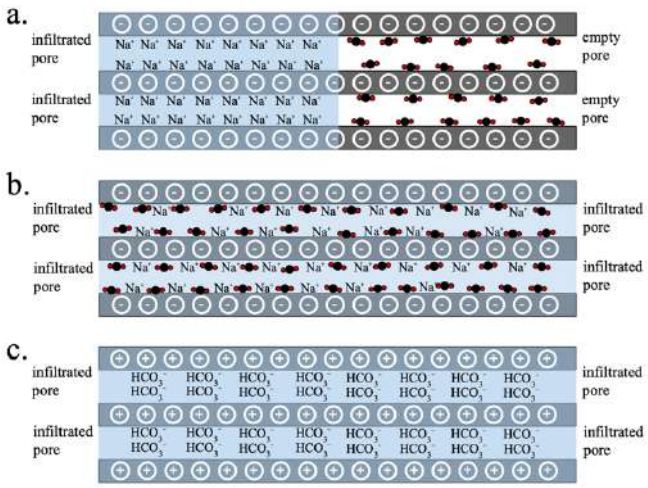

Figure 1. (a) adsorption of gas molecules at the gas-solid interface (b) adsorption of gas molecules at the gas-liquid interface (c) adsorption of ionized gas molecules at the gas-liquid interface

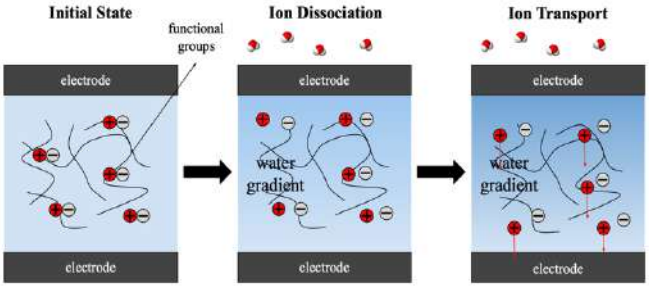

Figure 2. Schematic of the mechanism of a water gradient-based moisture electricity generation

Supercapacitive swing adsorption (SSA) is a relatively

new approach to carbon capture technology, developed by researchers at Lehigh University in 2014 [16, 17]. SSA is a form of electrochemical swing adsorption technology, as it enables selective and reversible adsorption and desorption of CO_2 through charge/discharge cycles of a supercapacitor, with one electrode in contact with the CO_2 containing gas, while the other is completely immersed in the electrolyte [16]. SSA has been observed in several electrolytes, including sodium chloride (NaCl), lithium chloride (LiCl), potassium chloride (KCl), and other chlorides [18]. SSA is environmentally friendly as it only requires carbon electrodes and NaCl, and the whole process is energy efficient as the charge discharge cycle wastes little energy. However, the relatively small amount of CO_2 adsorption capacity is the main challenge of this technology, with the maximum CO_2 adsorption reported 524 mmol kg^{-1} [20]. Amine scrubbing in comparison has an average adsorption capacity of about 3 mol kg^{-1} [19]. This challenge is mainly associated with the lack of fundamental understanding behind the principles of the SSA of CO_2 [13]. Recent attempts have been made by several researchers to increase the understanding of the mechanisms behind SSA. In 2019, Zhu et al. experimented the relations between electrolyte concentration and the SSA of CO_2 and proposed three possible mechanisms: (a) adsorption of gas molecules at the gas-solid interface, (b) adsorption of gas molecules at the gas-liquid interface, and (c) adsorption of ionized gas molecules (CO_2^-) at the gas-liquid interface (Figure 1) [18]. In 2022, Binford et al. attempted to further investigate the mechanisms underlying SSA by experimenting new charging protocols with new experimental methods [13]. In 2023, Bilal et al. explored the relationship between the voltage performance of SSA of CO_2 [20]. Although SSA requires substantially less energy and resources than other CCS technologies, the initial challenge revolving energy consumption is not solved. Herein, this study presents a novel approach to SSA with a novel thin-film moisture electricity generator (MEG) in a supercapacitor structure. If a new supercapacitor powered by green energy that consumes CO_2 during charge/discharge cycles is developed, it would substantially reduce CO_2 concentrations in the atmosphere with additional energy production.

The new generation of third energy storage (3rd-ES) technologies is a highly promising technology of the future. For decades, energy storage devices have been relying on external power sources that harvests energy [21]. Recently, moisture-electricity generation has received attention as a new source of green energy due to its abundance in nature [22-24]. One mechanism of moisture electricity generation utilizes a water gradient within the solid-state electrolyte as shown in (Figure 2) [25]. The CO_2 adsorbing MEG device developed by this study utilizes this water gradient to generate green electricity. When ambient moisture is absorbed by the hygroscopic material within the supercapacitor, the ionic material embedded in the electrolyte undergoes ionization, releasing numerous charged ions. Due to the design of the MEG, moisture only enters from top electrode and creates an uneven distribution of moisture and an ionization gradient, which drives the microfluidic or nanofluidic water transport in thin films that creates charge transport within the supercapacitor [26]. With the generated electric field, the developed device captures CO_2 via SSA as it adsorbs and separates CO_2 using a change in electrical potential.

2. Materials and Methods

2.1 Materials

Graphene nanoplatelets (EG016; 50 nm-5 μm diameter, sheet resistivity of < 10 ohm/square, surface area of < 250 m^2 per gram, mono-, bi-, and tri-layer content: > 85%) were supplied from Celtig (TN, USA). Super P conductive carbon black was purchased from MTI Korea. Poly (viny alcohol) (PVA; weight-averaged molecular mass (Mw)~ 13,000-23,000, 87-89% hydrolyzed), polytetrafluoroethylene (PTFE; 60wt% dispersion in H_2O), polyvinylidene fluoride (PVDF), sodium nitrate ($NaNO_3$), potassium permanganate ($KMnO_4$) were purchased from Sigma Aldrich. Sulfuric acid (H_2SO_4; 95-97%) and hydrogen peroxide (H_2O_2; 28%) were purchased from Duksan Pure Chemicals. N-Methyl-2-pyrrolidone (NMP; 99%) was purchased from Junsei Chemical. Sodium chloride (NaCl) was derived from evaporating the sea water obtained from the coast of Busan, South Korea.

2.2 Synthesis of Graphene Oxide

Graphene oxide (GO) was prepared by chemically processing graphene nanoplatelets according to the modified Hummer's Method [27]. 5 g of graphene nanoplatelet was mixed with 2.5 g of $NaNO_3$ and 115 mL of H_2SO_4 (95-97%) by stirring for 30 min in an ice bath. 15 g of $KMnO_4$ was slowly added to the flask and the mixture was stirred for 30 min at 35°C. The glass flask was then placed in an oil bath and a reflux assembly and 500 mL of deionized water was slowly added to the mixture, slowly raising the temperature to 90°C. To terminate the reaction, 10 mL of H_2O_2 (30%) was added.

After the mixture cooled down to room temperature, the remaining graphene powder was washed with deionized water by using a centrifuge (5 cycles; 30 min; 4000 rpm).

The mixture was then ice sonicated with a Power Sonic 505 (Hwashin Technology; 40 KHz, 10°C) for 20 minutes to ensure equal dispersion of GO in H_2O. The resulting GO dispersion (5.7 mg/g, dispersion in H_2O) was characterized by evaporating the solvent and calculating the weight difference of the samples.

2.3 Fabrication of Composites

The bottom electrode was created by mixing PVDF, super p, and NMP in a weight ratio of 4:1:30 for 30 min with a mortar. The created mixture was in the form of a slurry, and the slurry was coated with a thickness of 25 μm on a 15 μm copper foil with a doctor blade. like a wallet. The film was dried at room temperature overnight, and the resulting film's thickness was around 200 μm.

A PVA/NaCl solid-state electrolyte was obtained by stirring 4 g PVA in 40 mL distilled water at 110°C for 1h with the beaker covered with aluminum foil. 1 g of NaCl was then added to the mixture and the mixture was rigorously stirred at 90°C for 2 h. The aluminum foil was removed, and the mixture was stirred at 80°C for 1h to evaporate the solvent until the mixture became a slurry. The mixture then was cooled down to temperature for 48 h to remove any bubbles created during the process.

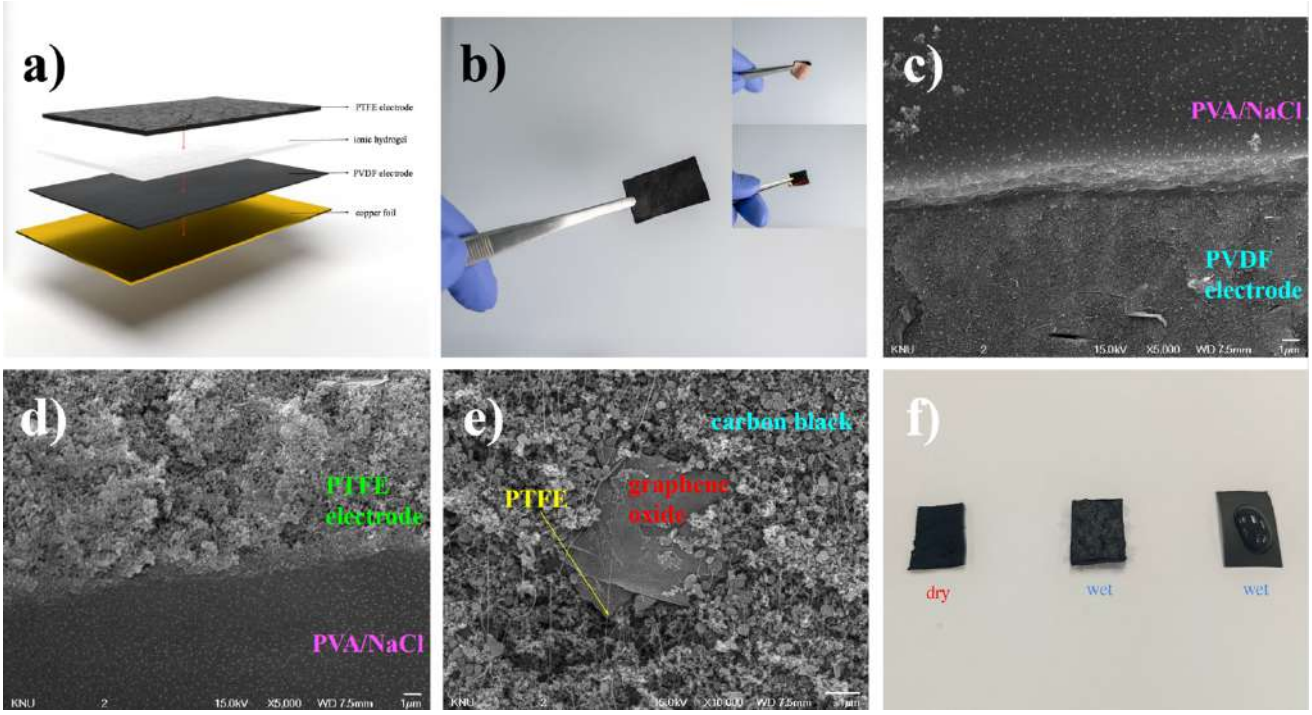

Figure 3. (a) 3D schematic of the structure of the thin-film supercapacitor. (b) Photograph of the assembled device and demonstration of its flexibility. (c) Cross-section scanning electron microscope (SEM) image between the PVA/NaCl layer and the PVDF electrode. (d) Cross-section SEM image between the PVA/NaCl layer and the PTFE electrode. (e) High-quality SEM image showing PTFE/Super P/ GO film. The GO is embedded in carbon black, and PTFE is the silk-looking material that bonds the material together. (f) Photograph of a dry PTFE film (left), wet PTFE film (middle), and a wet PVDF film (right).

The top electrode was prepared by dissolving 3 g of PTFE dispersion solution into 20 mL of ethanol with 10 min of stirring and 10 min of sonication (40 KHz, 20°C). 0.5 g of Super P and 0.05 g of GO were added to the mixture and overnight at room temperature. The mixture was stirred for an additional time to evaporate the remaining solvent until the mixture became a dough like substance. The mixture was gathered into a single mass and was kneaded until the mixture was malleable. The mixture was placed on a glass sheet, and it was uniformly rolled out with a glass stirring rod. The carbon sheet was transferred with a razor blade to an aluminum foil, which was folded

2.4 Fabrication of MEG

The device was designed by the procedure illustrated in Figure 3a. The PVDF/Super P/GO mixture was coated on the copper foil with a doctor blade and dried in an oven for 1 h at 120°C to evaporate the remaining solvent. The sample was then coated with PVA/NaCl gel in the same method, and dried in an oven for 1h at 80°C. After cooling down, the sample was cut into a 1 cm × 1 cm square. To firmly attach the PTFE electrode to the sample, one drop of deionized water was dropped above the sample with a pipette and spread out to partially dissolve the PVA/NaCl mixture before the PTFE film was attached. After

assembling the device, the copper foil was easily peeled off the bottom electrode, increasing the flexibility of the device. Figure 3b shows an image of the finished device and demonstrates its flexibility.

2.5 Material Characterization

The relative humidity (RH) was measured with a hygrometer (SwitchBot Meter Plus). The experiment was conducted in a homemade chamber illustrated in Figure 4e. The RH of the chamber was controlled with a humidifier and silica gel (Kanto Chemical). The water absorption measurements of the hygroscopic PVA/NaCl layer were

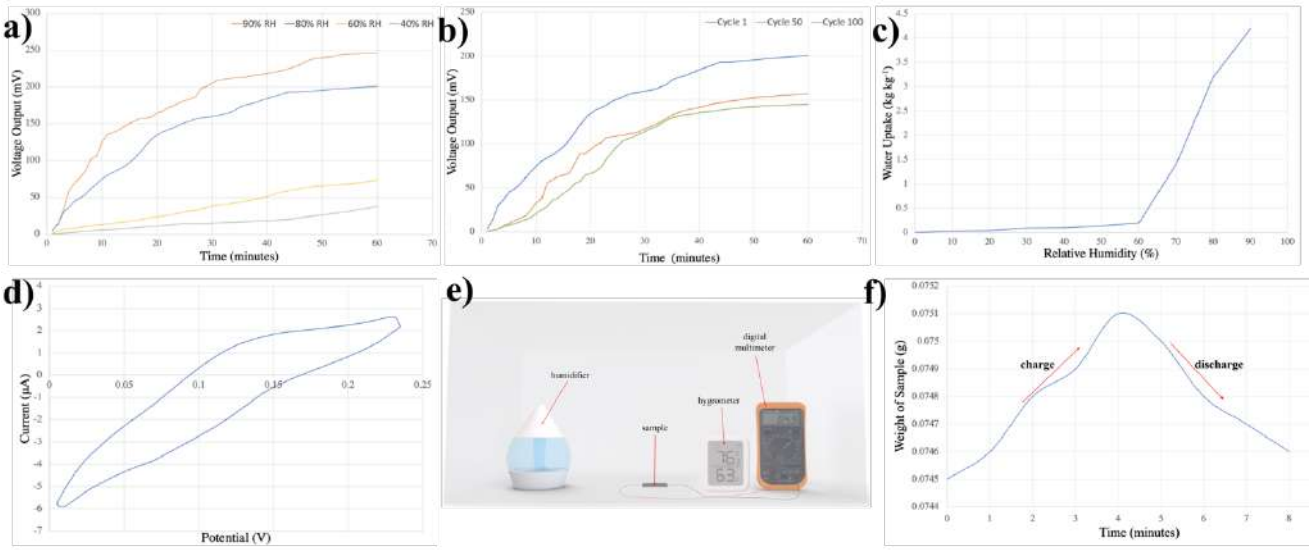

Figure 4. (a) Voltage output increases for 1h at 40%, 60%, 80%, 95% RH. (b) Voltage outputs for each cycle. (c) Amount of water uptake of ionic hygroscopic film for 3h at 10%, 20%, 30%, 40%, 50%, 60%, 70%, 80%, 90% RH. (d) Cyclic voltammetry curve of the device in the process of water absorption. Scan rate: 10 mV s^{-1}. (e) Schematic of the homemade humidity chamber for voltage output experiments. (f) Weight changes of the device during charge/discharge cycles.

To compare the wettability of the films, contact angle measurements were conducted. Micromorphology and structural characteristics of PVA/NaCl films, PVDF/Super P/GO films, and PTFE/Super P/GO films were characterized by field emission scanning electron microscope (FE-SEM; JEOL model JSM-6701F, Japan). PVA/NaCl samples were sputter coated (JEOL model JFC-1100E) with gold before scanned. The SEM images of the cross section of the PVA/NaCl and the electrode layers were taken by freezing the sample in liquid nitrogen and splitting the film. Energy dispersive x-ray spectroscopy (EDS; Hitachi SU8230) analysis was used to identify the sodium and chlorine elements to analyze the sea salt distribution throughout the PVA film.

2.6 MEG Performance Metrics

The voltage output, open-circuit voltage (V_{oc}), and short-circuit current (I_{oc}) of the device was measured with an electrochemical workstation (WonATech, ZIVE SP1) and a digital multimeter (Checkman, TK-4001). The sheet resistance of each film was also measured in real time with a digital multimeter (Checkman, TK-4001). The cyclic voltammetry (CV) curves of the MEG were measured with a battery tester 10 channel (WonATech, WBCS3000).

calculated via the net mass changes of the sample. The weight of each sample was measured with an electronic balance (Mettler Toledo, MS204S). Before testing, all samples were dehydrated in a furnace at 30°C for 12 h, and each sample was left in the chamber for 5 min, 15 min, 6 h, 10 h in 95%, 80%, 60%, 40% RH respectively before testing to wet the electrode before measuring electric output.

2.7 SSA Performance Metrics

The experiment was conducted within an electronic balance (Mettler Toledo, MS204S) in a room with a constant temperature of 25°C. 15% CO_2/ 85% N_2 gas mixture and moisture via a humidifier was flowed into the electronic balance for 30 minutes to match the chamber's CO_2 levels to 15% and the RH to 80% to mimic flue gas. After exposing the device to moisture for 1 hour, completely saturating the hygroscopic material, the device was connected to a battery tester to simulate charge/discharge cycles of the supercapacitor.

During the charge/discharge cycles of the device, the weight of the device was constantly monitored and measured. Pure N_2 gas was used for the control experiment with the identical procedure. The overall adsorption capacity

was taken as the mean of adsorption capacities for each cycle.

3. Results and Discussion

3.1 Electric Output

The different voltage outputs (mV) for relative humidities (RH; 40%, 60%, 80%, 95%) are shown in Figure 4a. The maximum voltage output of a single sample reached was 0.24 V after 1h at a RH of 95% and a short circuit of a several microamperes. The results show the device generates less energy when the RH is lower, and the voltage output of the device significantly increases when the RH is higher than 60%. This is fact is also supported by Figure 4c, which depicts the amount of water uptake of the hygroscopic PVA/NaCl film. Results show sharp increases in the amount of water absorbed in RHs higher than 60%. The more amount of water absorbed means faster development of a water gradient and more ionization of NaCl. Therefore, the higher water uptake highly correlates with the voltage output of the device. The device's cycle stability was also good, with the device's performance maintaining 80% of the first cycle after 100 cycles (Figure 4b). The device's capacitance was calculated as 0.02 Fg^{-1} with the CV curve in Figure 4d.

When ambient moisture is absorbed by the hygroscopic layer in the CO_2 adsorbing MEG, the NaCl embedded in the electrolyte undergoes ionization, releasing numerous charged ions. Because of the design of the MEG, moisture only enters from the top electrode and creates an uneven distribution of moisture and an ionization gradient, which drives the directional flow of ions within the MEG. This ionization also creates a spontaneous formation of an electrical double layer (EDL) between the electrodes and the electrolyte, which is confirmed by the CV curves of the device, creating a potential difference between the top and bottom electrodes (Figure 4d). CV tests (scan rate: 10 mVs^{-1}) were performed on a fully absorbed CO_2 adsorbing MEG based on a two-electrode configuration to further confirm the capacitive induced by an electric double layer (EDL). The cyclic voltammetry curve of the device shows a typical curve of a capacitor, which suggests no redox reactions were involved in the MEG. As the results show, the developed CO_2 adsorbing MEG device behaves like a capacitor upon water uptake. PVA was selected as the hygroscopic material as PVA film exerts high mechanical strength, high flexibility, and superior hygroscopicity [28-30]. PVA is also one of the few polymers that is biodegradable in nature [31]. Sea salt was selected as the ionic water absorbing material due to its eco-friendliness, cost, and good hygroscopicity [32]. The water absorption measurements showed exceedingly high water uptake capacity of the PVA film, reaching 400% of the weight of the water absorbing materials in the film (Figure 4c). The NaCl in the PVA film was also dispersed equally, as shown in Figure 5. PTFE was chosen as the binder for the top electrode as its film's physical properties enables water and CO_2 transport between the electrolyte and the electrode. The PTFE/Super P/GO film's high porosity allows wettability in water, and good film creating abilities increases the mechanical strength of the film [33]. Figure 6 demonstrates the wettability of the PTFE film. As shown in the figure, the top electrode fully absorbed water in 90 seconds whereas the bottom electrode did not.

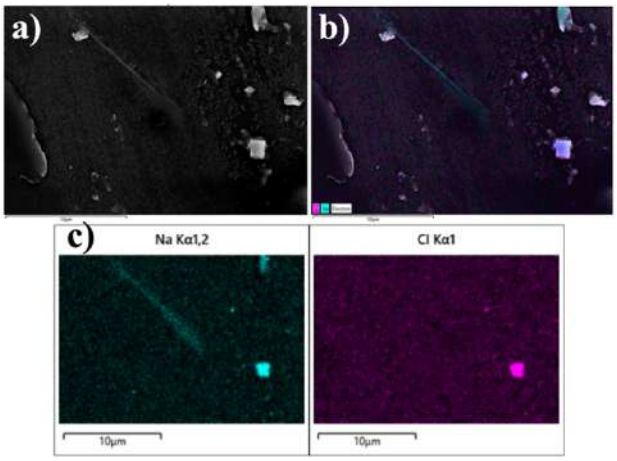

Figure 5. (a) High-quality SEM image of PVA/NaCl film. (b) EDS layered of the PVA/NaCl film. (c) EDS element mapping image showing the even distribution of Na and Cl elements throughout the film.

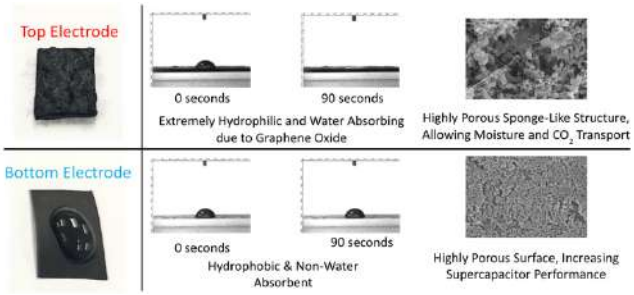

Figure 6. A table highlighting the characteristics of the top and bottom electrodes respectively.

This is due to the extremely porous sponge-like structure of the PTFE film due to the film's low density and relatively high PTFE wt% in the film. The film has a relatively low density because of the absence of the roll pressing process, which is a typical step in battery manufacturing. Roll pressing increases an electrode's density and evenly flats the electrode, but the increased density worsens an electrode's wettability. To further increase

Figure 7. (a) 3D schematic of a real-life application of the device in CO_2 producing facilities. (b) 3D schematic of the device integrated with building facades. (c) 3D schematic of the device being utilized in integrated urban planning to reduce urban carbon footprint.

the hydrophilicity of the top electrode, GO was also added [34]. Supporting Information 1 and 2 demonstrates how the addition of GO in the top electrode significantly increases the water adsorption capacity and wettability of the film. Figure 3e shows a homogenous structure of the GO and the PTFE/super p mixture. Although the PTFE film exerted great wettability in water due to the highly porous structure, PTFE is a hydrophobic material on its own, and increased hydrophilicity of the top electrode will help facilitate a quicker formation of a water gradient [35]. By allowing water and CO_2 to enter and leave the electrode freely, ambient moisture and CO_2 can be absorbed by the electrolyte. GO, however, is an insulator. The PTFE film without GO had a sheet resistance of about 30 Ω whereas the GO embedded film had a resistance of 40 Ω. GO, however, was still chosen as the hydrophilic material in the electrode because of its superior electrochemical characteristics. GO is famous for its abundance in oxygen containing functional groups [36]. Such functional groups are important in increasing the performance of the device as dissociation of functional groups upon water uptake releases numerous charged ions that create a directional flow within the electrolyte [37]. PVDF was chosen as the binder for the bottom electrode due to its super hydrophobic properties (Figure 3f) [38, 39]. For a water gradient to form, moisture needs to enter from one side, whereas the other electrode is completely sealed [40]. Water absorption on both ends would create complete saturation, therefore generating no energy. Water absorption in humid environments for long periods of time would also lead to complete saturation. Figure 3c and Figure 3d shows that the two electrode layers (PVDF & PTFE) are well attached to the electrolyte layer. The PTFE film was attached to the electrolyte layer by partially melting the PVA film with deionized water and pressing the PTFE film on the PVA film, and the SEM image of the cross-section between the PTFE layer and the PVA layer confirms good adhesion between the two layers (Figure 3c).

3.2 CO_2 Adsorption Capacity

Figure 4f shows the weight changes of the supercapacitor during charge/discharge cycles. An increase of 0.0005 g was observed during charge/discharge cycles and the reversibility of the CO_2 adsorption was shown through the decrease in device weight as the supercapacitor discharged. The adsorbed gas was confirmed to be CO_2 as the control experiment with pure N_2 gas showed no meaningful weight increases. CO_2 adsorption upon multiple cycles is also observed. By converting grams into moles of CO_2, the CO_2 adsorption capacity was observed to be approximately 0.0118 mmol per 1 cm^2, and 0.15 mol per kg^{-1}.

The SSA mechanism of this device can be explained by the theories presented in Figure 1. The design of the CO_2 adsorbing moisture powered supercapacitor, especially the fabrication process, is crucial for SSA to happen. Coating the copper foil with PVDF and coating PVA/NaCl gel on the PVDF layer allowed the hygroscopic ionic gel to fully penetrate into the PVDF layer. This allows the structure to mimic that of the SSA supercapacitor cell, where one electrode is completely immersed in the electrolyte, while the other is in contact with the CO_2 containing gas. The developed samples' CO_2 adsorption was identified by comparing the pressure changes of the chamber with a CO_2/N_2 gas and pure N_2 gas. The control experiment with pure N_2 confirmed the adsorbed gas was CO_2. In fact, a study by B. Kokoszka et al. measured slight pressure increases of 0.5 Torr in a sealed container with pure N_2 gas during a supercapacitor's charge/discharge cycles, suggesting N_2 is repelled by the supercapacitor [17].

3.4 Future Applications

This novel moisture powered thin-film supercapacitor

has numerous applications in the real world. Due to its thin and flexible form factor, the device is applicable on irregular geometries and is scalable due to the relatively low cost of the raw materials. Thus, in CO_2 producing facilities where CO_2 capture technology is used the most, the device can be easily integrated into its flue gas filtering system. Flue gas, typically a moist CO_2 containing gas [41], enters the cross-section of the pipe shown in the diagram with the flexible CO_2 adsorbing supercapacitors attached to the walls of the pipe (Figure 7a). The device captures carbon dioxide while producing additional green energy from an already existing source. As depicted in Figures 6b and 6c, potential uses also include environmental applications where the device could be integrated into structures or materials exposed to the atmosphere, such as building facades or street lamps, allowing for passive carbon capture in everyday settings. This would contribute to reducing the overall carbon footprint without requiring additional energy input. The flexible and scalable nature of this device would allow for widespread use of carbon capture technologies in everyday life, and the manufacturing process of this device which is similar to that of conventional battery manufacturing processes allows for immediate mass production an commercialization of this device.

However, scaling up the power output of the device is necessary due to its low output (0.24V, 2.5μA), but is achievable by connecting multiple devices in series or parallel. There are two systems for power output from this device. First, the device can be connected to a capacitor or battery to store the generated electricity. Second, the device can be used for direct energy supply. Figure 7c demonstrates 4 naturally charged devices connected in series directly powering an LED.

The previously reported systems for carbon capture require substantial amount of energy, requires large facilities, or extremely toxic to the environment. [Table 1] summarizes conventional types of carbon capture technology and the newly discovered field of energy generating carbon capture technology with this study. With this technology being moisture powered, the developed supercapacitor can power a device while capturing CO_2. Given that the approach proposed by this study can be effectively applied to various conductive and active materials, this study suggest that this approach can provide a facile and versatile basis for designing highly efficient and practical carbon capture technologies.

Table 1. Comparison of the efficiency and practicality of carbon capture technologies [9-17, 42, 43]

Type	Energy Consumption	Availability
Chemical Adsorption	High	Requires specialized facilities, toxic chemicals used
Physical Adsorption	Moderate	Requires specialized facilities
Cryogenic Processes	High	Requires specialized facilities
Membrane Processes	Low	Relatively compact but requires a stream of air
Supercapacitive Swing Adsorption (energy consuming)	Low	Requires a fuel cell module to adsorb CO_2
Energy Generating Supercapacitive Swing Adsorption (this study)	No energy consumed, generates energy	Usable in almost any environment or application

4. Conclusion

In summary, this study demonstrated a novel approach to carbon capture by implementing SSA into a thin-film moisture electricity generator. The developed thin-film supercapacitor successfully demonstrated the capacity for supercapacitive swing adsorption of CO_2, which is a relatively novel approach to CCS that is cheap, environmentally friendly, and efficient while generating green energy from ambient humidity. The materials used as the binder for the two electrodes successfully act as hydrophilic and hydrophobic layers, which was crucial for the formation of a water gradient within the ionic hygroscopic layer. Upon full water uptake, the voltage output would decrease back to 0, until the absorbed water evaporates, and new moisture enters the device. When exposed to a humid environment after water desorption, the supercapacitor would recharge and harvest energy from ambient environments in a cyclic operation mode. The device also exhibit good cycle stability as the device retains ~80% of its original output after 100 cycles. With a novel approach that combines thin-film moisture electricity generation with supercapacitive swing adsorption, this work not only inspires the designs of SSA device fabrication but also advances the efficiency and practicality of carbon capture technologies.

References

[1] K. Abbass, M. Qasim, H. Song, M. Murshed, H. Mahmood, I. Younis, “A review of the global climate

change impacts, adaptation, and sustainable mitigation measures", *Environmental Science and Pollution Research*, 29(28), pp. 42539–42559, April, 2022.

[2] S. Chu, Y. Cui, N. Liu, "The path towards sustainable energy", *Nature Materials*, 16(1), pp. 16–22, December, 2016.

[3] M. Venkataramanan, "Causes and effects of global warming", *Indian Journal of Science and Technology*, 4(3), pp. 226–229, 2011.

[4] R. B. Alley, J. Marotzke, W. Nordhaus, J. T. Overpeck, D. M. Peteet, R. A. Pielke, R. T. Pierrehumbert, P. B. Rhines, T. F. Stocker, L. D. Talley, J. M. Wallace, "Abrupt Climate Change", *Science*, 299(5615), pp. 2005–2010, March, 2003.

[5] J. Lelieveld, K. Klingmüller, A. Pozzer, R. T. Burnett, A. Haines, V. Ramanathan, "Effects of fossil fuel and total anthropogenic emission removal on public health and climate", *Proceedings of the National Academy of Sciences of the United States of America*, 116(15), pp. 7192–7197, March, 2019.

[6] S. W. Pacala, R. H. Socolow, "Stabilization Wedges: Solving the Climate Problem for the Next 50 Years with Current Technologies", *Science*, 305(5686), pp. 968-972, August, 2004.

[7] M. I. Hoffert, K. Caldeira, G. Benford, D. R. Criswell, C. Green, H. Herzog, A. K. Jain, H. S. Kheshgi, K. S. Lackner, J. S. Lewis, H. D. Light-foot, Manheimer, W. Manheimer, J. C. Mankins, M. E. Mauel, L. J. Perkins, M. E. Schlesinger, T. Volk, T. M. L. Wigley, "Advanced Technology Paths to Global Climate Stability: Energy for a Greenhouse Planet", *Science*, 298(5595), pp. 981–987, November, 2002.

[8] G. T. Rochelle, "Amine Scrubbing for CO_2 Capture", *Science*, 325, pp. 1652-1654, September, 2009.

[9] L. Fu, Z. Ren, W. Si, M. Qian, W. Huang, K. Liao, Z. Huang, Y. Wang, J. Li, P. Xu, "Research progress on CO_2 capture and utilization technology", *Journal of CO_2 Utilization,* 66, pp. 102260–102260, December, 2022.

[10] Z. Yang, B. Lu, D. Guo, Z. Ji, C. Ji, G. Zhang, "Research status and progress of CO_2 capture and separation methods", *Shandong Chemical Industry*, 49(18), pp. 62-64, 2020.

[11] J. Cai, Y. Zhang, C. G. Xu, Z. M. Xia, Z. Y. Chen, X. S. Li, "Raman spectroscopic studies on carbon dioxide separation from fuel gas via clathrate hydrate in the presence of tetrahydrofuran", *Applied Energy*, 214, pp. 92-102, March, 2018.

[12] L. X. Hao, G. J. Zhang, Y. Jia, J. W. Qu, A. T. Su, "Progress of CO_2 adsorption performance of solid porous materials", *Modern Chemical Industry*, 36(07), pp. 29-32, July, 2016.

[13] T. B. Binford, G. Mapstone, I. Temprano, A. C. Forse, "Enhancing the capacity of supercapacitive swing adsorption CO_2 capture by tuning charging protocols", *Nanoscale*, 14(22), pp. 7980–7984, May, 2022.

[14] J. S. Kang, S. Kim, T. A. Hatton, "Redox-responsive sorbents and mediators for electrochemically based CO_2 capture", *Current Opinion in Green and Sustainable Chemistry*, 31, pp. 100504–100504, October 2021.

[15] M. Rahimi, G. Catalini, M. Puccini, T. A. Hatton, "Bench-scale demonstration of CO_2 capture with an electrochemically driven proton concentration process", *RSC Advances*, 10(29), pp. 16832–16843, April, 2020.

[16] K. Landskron, "Capacitance for Carbon Capture", *Angewandte Chemie International Edition*, 57(14), pp. 3548–3550. February, 2018.

[17] B. Kokoszka, N. K. Jarrah, C. Liu, D. T. Moore, K. Landskron, "Supercapacitive Swing Adsorption of Carbon Dioxide", *Angewandte Chemie International Edition*, 53(14), pp. 3698–3701, February, 2014.

[18] S. Zhu, J. Li, A. Toth, and K. Landskron, "Relationships between Electrolyte Concentration and the Supercapacitive Swing Adsorption of CO_2", *ACS Applied Materials & Interfaces*, 11(24), pp. 21489-21495, May, 2019.

[19] P. Brœder, H. F. Svendsen, "Capacity and Kinetics of Solvents for Post-Combustion CO_2 Capture", *Energy Procedia*, 23, pp. 45–54, 2012.

[20] M. Bilal, J. Li, H. Guo, K. Landskron, "High-Voltage Supercapacitive Swing Adsorption of Carbon Dioxide", *Small*, 19(24), June, 2023.

[21] J. Ling, R. Kunwar, L. Li, S. Peng, I. I. Misnon, M. H. A. Rahim, C. C. Yang, R. Jose, "Self-rechargeable energizers for sustainability", *EScience*, 2(4), pp. 347–364, July 2022.

[22] X. Liu, H. Gao, J. E. Ward, B. Yin, T. Fu, J. Chen, D. R. Lovley, J. Yao, "Power generation from ambient humidity using protein nanowires", *Nature*, 578(7796), pp. 550–554, February, 2020.

[23] D. Champier, "Thermoelectric generators: a review of applications", *Energy Conversion and Management*. 140, pp. 167–181. May, 2017.

[24] Z. L. Wang, "Triboelectric nanogenerators as new energy technology for self-powered systems and active mechanical and chemical sensors", *ACS Nano*, 7(11), pp. 9533–9557, September, 2013.

[25] Z. Sun, X. Wen, L. Wang, D. Ji, X. Qin, J. Yu, S.

Ramakrishna, “Emerging design principles, materials, and applications for moisture-enabled electric generation”, *EScience*, 2(1), pp. 32–46, January, 2022.

[26] G. Xue, Y. X, T. Ding, J. Li, J. Yin, W. Fei, Y. Cao, J. Yu, L. Yuan, L. Gong, J. Chen, S. Deng, J. Zhou, “Water-evaporation-induced electricity with nanostructured carbon materials”, *Nature Nanotechnology*. 12, pp. 317–321, January, 2017.

[27] N. I. Zaaba, K. L. Foo, U. Hashim, S. J. Tan, Wei-Wen Liu, C. H. Voon, “Synthesis of Graphene Oxide using Modified Hummers Method: Solvent Influence”, *Advances in Material & Processing Technologies Conference*, April, 2017.

[28] T. D. Bui, Y. Wong, K. Thu, S. J. Oh, M. K. Ja, K. C. Ng, I. Raisul, K. J. Chua, “Effect of hygroscopic materials on water vapor permeation and dehumidification performance of poly(vinyl alcohol) membranes”, *Journal of Applied Polymer Science*, 134(17), pp. 44765, January, 2017.

[29] E. Yang, X. Qin, S. Wang, “Electrospun crosslinked polyvinyl alcohol membrane”, *Materials Letters*, 62(20), pp. 3555–3557, July, 2008.

[30] H. Zhang, Q. Wang, L. Li, “Dehydration of water-plasticized poly(vinyl alcohol) systems: particular behavior of isothermal mass transfer”, *Polymer International*, 58(1), pp. 97–104, November, 2008.

[31] X. Tang, S. Alavi, “Recent advances in starch, polyvinyl alcohol based polymer blends, nanocomposites and their biodegradability” *Carbohydrate Polymers*, 85(1), pp. 7–16, April, 2011.

[32] Y. Zhang, S. Guo, Z. G. Yu, H. Qu, W. Sun, J. Yang, J. Suresh, X. Zhang, J. J. Koh, S. C. Tan, “An Asymmetric Hygroscopic Structure for Moisture-Driven Hygro-Ionic Electricity Generation and Storage”, *Advanced Materials*, 34(21), March, 2022.

[33] J. Y. Lee, D. P. Lim, D. S. Lim. “Tribological behavior of PTFE nanocomposite films reinforced with carbon nanoparticles”, *Composites Part B: Engineering*, 38(7-8), pp. 810–816, October, 2007.

[34] G. Wang, B. Wang, J. Park, J. Yang, X. Shen, J. Yao, “Synthesis of enhanced hydrophilic and hydrophobic graphene oxide nanosheets by a solvothermal method”, *Carbon*, 47(1), pp. 68–72. January, 2009.

[35] A. Mondal, R. Devine, L. Estes, J. Manuel, P. Singha, J. Mancha, M. Palmer, H. Handa, “Highly hydrophobic polytetrafluoroethylene particle immobilization via polydopamine anchor layer on nitric oxide releasing polymer for biomedical applications”, *Journal of Colloid and Interface Science*, 585, pp. 716–728, March, 2021.

[36] E. Aliyev, V. Filiz, M. M. Khan, Y. J. Lee, C. Abetz, V. Abetz. “Structural Characterization of Graphene Oxide: Surface Functional Groups and Fractionated Oxidative Debris”, *Nanomaterials*, 9(8), pp. 1180, August, 2019.

[37] R. Zhu, Y. Zhu, F. Chen, R. Patterson, Y. Zhou, T. Wan, L. Hu, T. Wu, R. Joshi, M. Li, C. Cazorla, Y. Lu, Z. Han, D. Chu, “Boosting moisture induced electricity generation from graphene oxide through engineering oxygen-based functional groups”, *Nano Energy*, 94, pp. 106942, April, 2022.

[38] R. P. S. Chakradhar, G. Prasad, P. Bera, C. Anandan. “Stable superhydrophobic coatings using PVDF–MWCNT nanocomposite”, *Applied Surface Science*, 301, pp. 208–215, May, 2014.

[39] D. Hou, J. Wang, D. Qu, Z. Luan, X. Ren, “Fabrication and characterization of hydrophobic PVDF hollow fiber membranes for desalination through direct contact membrane distillation”, *Separation and Purification Technology,* 69(1), pp. 78–86, September, 2009.

[40] D. Shen, W. W. Duley, P. Peng, M. Xiao, J. Feng, L. Liu, G. Zou, Y. Zhou, “Moisture-Enabled Electricity Generation: From Physics and Materials to Self-Powered Applications”, *Advanced Materials*, 32(52), November, 2020.

[41] Tai T.T. Nguyen, J.-B. Lin, George K.H. Shimizu, and A. Rajendran, “Separation of CO2 and N2 on a hydrophobic metal organic framework CALF-20,” Chemical engineering journal, vol. 442, pp. 136263–136263, Aug. 2022, doi: https://doi.org/10.1016/j.cej.2022.136263.

[42] United States Government Accountability Office. Decarbonization Status, Challenges, and Policy Options for Carbon Capture, Utilization, and Storage Accessible Version. Government Accountability Office, 2022, Available From: https://www.gao.gov/assets/730/723198.pdf. (accessed Nov., 17, 2023)

[43] S. Vaz, A. P. R. Souza, B. E. L. Baeta, “Technologies for carbon dioxide capture: A review applied to energy sectors”, *Cleaner Engineering and Technology*, 8, pp. 100456, June 2022.

Acknowledgements

All experiments were conducted in Kyungpook National University. The author would like to thank Professor Yeon Uk Jeong for his support and guidance throughout the research process.

Supporting Information

[1] Movie of the contact angle test of the top electrode with graphene oxide: https://youtu.be/R9b4tFxmS_4
[2] Movie of the contact angle test of the top electrode without graphene oxide: https://youtu.be/eRIXxi006UM
[3] Movie of the contact angle test of the bottom electrode: https://youtu.be/EamZzRFIL60

【評語】100045

The research addresses a critical global issue—carbon dioxide emissions and climate change. It effectively highlights the limitations of current carbon capture and storage (CCS) technologies, making a strong case for the need for innovative solutions. Some comments are raised accordingly.

1. The discussion on integrating the device into existing infrastructure (e.g., flue gas systems, and building facades) is promising. This could lead to significant reductions in carbon footprints in urban settings.
2. While the device shows potential, the need to enhance power output is acknowledged. Suggestions for connecting multiple devices in series or parallel are practical and feasible.
3. Future work should focus on optimizing power output and exploring commercial viability.